Available online at www.sciencedirect.com
SCIENCE DIRECT®

Journal of the European Ceramic Society 24 (2004) 693–698

www.elsevier.com/locate/jeurceramsoc

Thermogravimetric and thermokinetic investigation of the dehydroxylation of a hydroxyapatite powder

Tao Wang*, Annett Dorner-Reisel, Eberhard Müller

Institute of Ceramic Materials, Gustav-Zeuner-Straße 3, Freiberg University of Mining and Technology, 09596, Freiberg, Germany

Received 21 November 2002; received in revised form 11 February 2003; accepted 6 April 2003

Abstract

The dehydroxylation of HA powder was investigated using thermogravimetric analysis over the range of room temperature to 1250 °C. The kinetic result of dehydroxylation of HA was calculated by means of the Ozawa–Flynn–Wall method. According to calculated activation energy-conversion degree plot, the kinetics of HA dehydroxylation was identified as a comprehensive one, which included four reaction-rate-controlling processes with different activation energies and four successive conversion stages kinetically controlled by different rate-controlling processes. These four reaction-rate-controlling processes were interpreted as OH^--anion diffusion through HA, OH^--anion debonding from HA lattice, the lattice constitution of OA, and $2OH^- \rightarrow H_2O\uparrow + O^{2-}$ at the reaction interface.

Keywords: Apatites; Dehydroxylation; DTG; Hydroxyapatite; Kinetics; TG

1. Introduction

Hydroxyapatite (HA) is a particularly attractive material, which has received considerable attention over the past two decades, for bone and tooth implants because of its chemical similarity to natural bone and excellent biocompatibility.[1,2] However, thermal decomposition of HA during the sintering of HA ceramics or processing of HA coatings yields in some undesirable influences on the physical, chemical, mechanical, and especially biomedical properties of HA products.[3] So the thermal behaviour of HA is of special importance for the application of HA for biomedical purposes.

The decomposition of HA includes two stages: dehydroxylation producing oxyapatite $Ca_{10}(PO_4)_6O$ (OA) after the appearance of hydroxyoxyapatite $Ca_{10}(PO_4)_6O_x(OH)_{2-2x}$ (OHA) as a transition product, and the following decomposition of OHA (and remained HA) resulting calcium phosphates.[3–6] Many researchers have studied thermal behaviour of HA ceramics and coatings. Unfortunately, their results, both initial temperatures for dehydroxylation and decomposition, and reaction formulas, are usually divergent due to the purity, crystallinity and the stoichiometry of HA, as well as the methods and the conditions employed in investigations. Recently both stages of the decomposition of stoichiometric HA were reported to be reversible under controlled heating and cooling conditions,[6–8] which results in some difficulties in kinetic studies on the thermal behaviour of HA. Moreover almost all reports were mainly focused on the decomposition stage, due to the judgement that the dehydroxylation stage has no significant effect on the properties of HA.[3–8] As known, the decomposition of HA is a process of continuous reactions, in which the conversion degree of dehydroxylation can strongly influence the critical temperature of subsequent decomposition. For example, the decomposition temperature of HA increased with the increasing water vapour pressure, by restricting dehydroxylation reaction.[3,4] So the kinetic investigation of dehydroxylation of HA should be regarded as the starting point for understanding the reaction kinetics of further decomposition on heating to higher temperatures.

Nowadays a variety of experimental methods have been used to explore the thermal behaviour of HA, e.g. X-ray Diffraction (XRD), Fourier Transform Infrared

* Corresponding author. Tel.: +49-3731-39-2085; fax: +49-3731-39-3662.
E-mail address: wang@ikw.tu-freiberg.de (T. Wang).

0955-2219/03/$ - see front matter © 2003 Elsevier Ltd. All rights reserved.
doi:10.1016/S0955-2219(03)00248-6

Spectroscopy (FTIR), Optical Microscopy, Scanning Electron Microscopy (SEM), Thermal analysis (TA, mainly including Thermogravimetry (TG), Differential Thermal Analysis (DTA) and Differential Scanning Calorimetry (DSC)), and Nuclear Magnetic Resonance (NMR).[3–11] Among them, TA method must be the most accurate and computationally available one for kinetic purposes, because of its characteristic real-time measurement and reliable thermo-kinetically computational methods. Especially, thermogravimetric methods, TG and Differential Thermogravimetry (DTG), are suitable techniques for characterization the dehydroxylation of HA.

Recently, the iso-conversional thermokinetic methods, mainly including the Ozawa–Flynn–Wall method, which has been incorporated into an American Society for Testing and Materials standard method, and Friedmann method,[12–26] were found to be effective in revealing the comprehensive kinetics of inhomogeneous solid-state reaction.[15–26] Namely, knowledge of the dependence of apparent activation energy (E) on conversional degree (α) assists in detecting both multiple processes and drawing certain mechanistic conclusions.[21–26] Using iso-conversional method, T. Wang et al.[27] have provided thermokinetic proofs for the diffusion-controlled reaction model of titanium aluminide synthesis reported by Wang and Dahms[28] based upon their metallurgical observations. In the present study, the dehydroxylation of HA was investigated by means of TG and DTG methods and its comprehensive kinetics were identified using the Ozawa–Flynn–Wall method.

2. Materials and methods

A commercial HA powder, Fluka brand (product of Sigma-Aldrich Chemie GmbH Munich, Germany), was used for the kinetic investigations of dehydroxylation. TG and DTA measurements were preceded with a STA-409C (NETZSCH-Gerätebau GmbH, Germany) simultaneous thermal analyzer. The heating temperature range is from room temperature to 1250 °C. The Al_2O_3 crucible, dried airflow at the rate of 100 cm^3/min and Al_2O_3 powder, as a reference sample, were applied in present TA experiments. About 100 mg HA powder was used and filled loosely in the crucible for every measurement. The thermokinetic calculation was conducted with the help of Thermokinetic software, developed by NETZSCH-Gerätebau GmbH, Germany, using the detected TG data.

3. Results and discussion

Fig. 1 shows the TG curves of Fluka HA powder at the heating rates of 2, 5, 10, 15 °C/min. According to the TG and DTG (in Fig. 2) curves, there are two mass loss stages: 100–500 °C and 680–1080 °C, on the heating process from room temperature to 1250 °C on these curves. The first mass loss process was reported as the removal of adsorbed water from the surface and pores.[29–32] Fig. 2 shows the DTG curves of the second mass loss stage, which corresponds to the dehydroxylation stage of decomposition of HA powder. At this stage, the percentage of the mass loss is about 1.44%, as shown in the conversion degree vs. temperature curve in Fig. 3, which amounts to 80% of the molar percentage of the H_2O molecule in a HA lattice. Also in Fig. 3, the temperature range of dehydroxylation of HA in the present study is 680–1080 °C, which agrees well with the previous TG result of another commercial HA powder reported by Adolfsson et al.,[33] Although 680 °C, the initial temperature of dehydroxylation, is a little bit lower than the previous reported values, which amounts to 800 °C or higher.[3–11] Such a temperature discrepancy

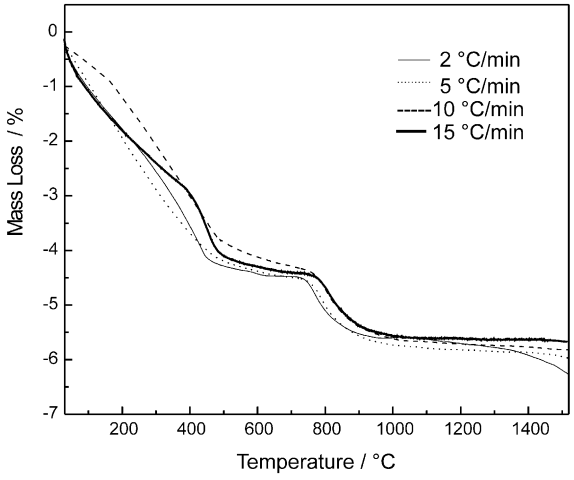

Fig 1. TG curves of Fluka HA powder at 2, 5, 10 and 15 °C/min.

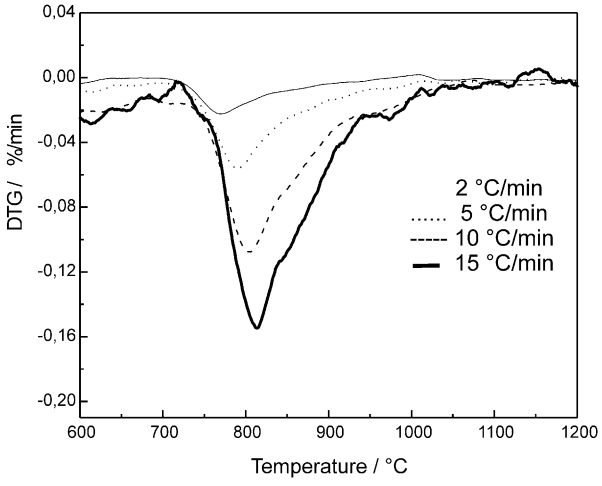

Fig 2. DTG curves of the dehydroxylation of Fluka HA powder at 2, 5, 10 and 15 °C/min.

should be attributed to the differences of samples and experimental methods, or even the partial rehydration during the quenching process for preserving the sample phase composition at elevated temperatures for some post-investigations.

Fig. 4 (a) and (b) show the E–α plot calculated using the Ozawa–Flynn–Wall method based on the TG data, and the schematic diagram of overall rate of mass loss of HA in 680–1080 °C. According to the characteristics of the E–α plot shown in Fig. 4(a), four activation energies can be identified: 190, 530, 410, and 235 kJ/mol belonging to four different kinetic processes: A ($0.02 \leqslant \alpha < 0.13$), B ($0.02 \leqslant \alpha < 0.7$), C ($0.13 \leqslant \alpha < 0.98$), and D ($0.8 \leqslant \alpha \leqslant 0.98$), respectively. Additionally, in the E–α plot, there are four successive conversion stages reflecting different dehydroxylation mechanisms: stage 1 ($0.02 \leqslant \alpha < 0.13$, 680 °C $\leqslant T <$ 764 °C), stage 2 ($0.13 \leqslant \alpha < 0.7$, 764 °C $\leqslant T <$ 866 °C), stage 3 ($0.7 \leqslant \alpha < 0.8$, 866 °C $\leqslant T <$ 897 °C), and stage 4 ($0.8 \leqslant \alpha \leqslant 0.98$, 897 °C $\leqslant T \leqslant$ 1080 °C), as plotted in Figs. 3 and 4.

The value of E at stage 1 varies from the value of process A to that of process B, which indicates the overall dehydroxylation rate at stage 1 is jointly controlled by both A and B according to the interpreting method of E–α plot,[21–26] as drawn in Fig. 4 (b). Similarly, the stages 2 and 4 are rate-controlled by processes B and C, as well as processes C and D. The dehydroxylation kinetics at stage 3 is quite different from those at the other stages. The E at stage 3 is constant, signifying this stage is only kinetically controlled by process C.[21–26]

3.1. Conversion stage 1 ($0.02 \leqslant \alpha < 0.13$, 680 °C $\leqslant$ T $<$ 764 °C)

Because of the gradual loss of water from the HA, OHA—a combination of HA and OA[4, 33–35] was formed.[3–11] Thereby, former OH^- positions were replaced by O^{2-} ions and vacancies. The conversion stage 1, as the initial stage of HA dehydroxylation, was widely reported proceeding as follows:

$$Ca_{10}(PO_4)_6(OH)_2 \rightarrow Ca_{10}(PO_4)_6(OH)_{2-2x}O_x + xH_2O \quad (1)$$

with $0 < x < 1$.[3–11]

For such an inhomogeneous solid-state reaction, there are at least five possible kinetic processes:

1. OH^--anion debonding from HA lattice;
2. OH^--anion diffusion through HA;
3. dehydroxylation reaction ($2OH^- \rightarrow H_2O\uparrow + O^{2-}$) at the reaction interface;
4. H_2O expulsion through product layer;
5. and the lattice constitution of OA.

The E values for OH^- diffusion in HA, and dehydroxylation reaction were reported to be 230[36] and 251 kJ/mol.[4] The so-called OHA is a combination of OA

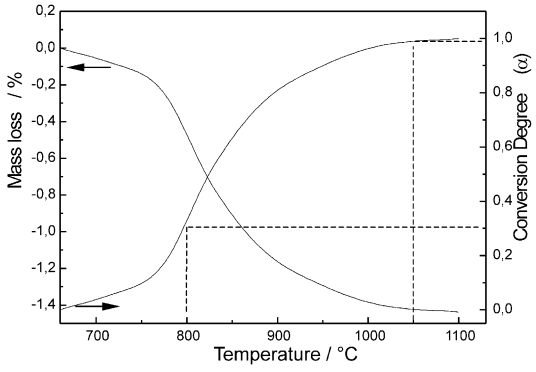

Fig. 3. The TG curve of the dehydroxylation process of Fluka HA powder at the heating rate of 10 °C/min and its conversion degree curve.

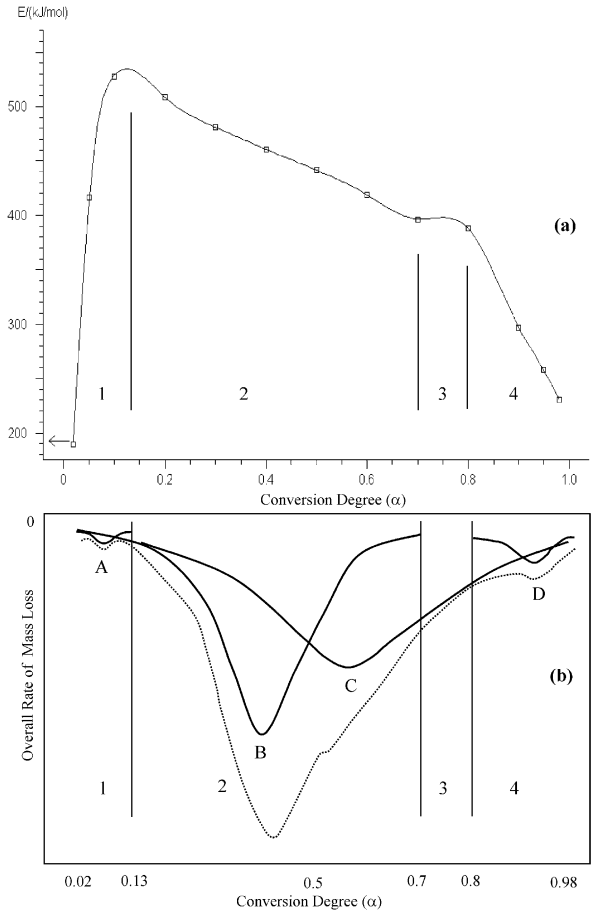

Fig. 4. E–α plot (a) calculated using the Ozawa–Flynn–Wall method and schematic diagram of overall rate of dehydroxylqation (b) of HA. The solid curves in (b) are the mass loss rates of process A, B, C and D, respectively, as well as the dash line drawn after the DTG curve at 15 °C/min, representing the overall rate of mass loss.

and HA,[4,33–35] thus the constitution of OHA lattice is actually the crystallization process of OA, i.e., the OA lattice constitution, which was reported as 440 kJ/mol.[36] Unfortunately, there is no quantitative report for the other two processes. The reported activation energies for the possible kinetic processes during the sintering of HA were listed in Table 1.

As stated above, the dehydroxylation within stage 1 is kinetically controlled by process A and B. By comparing the experimentally-detected values of E with reported ones, the process A has been found being of a similar E with OH^- diffusion through HA. Additionally, at the initial stage of dehydroxylation, the unreacted HA core remains in a considerable size. There are two possible routes for OH^- to diffuse through HA, radial diffusion from the interior of HA core to the reaction interface, and tangent diffusion from the OH^--rich areas to OH^--depleted areas within the OHA shell. For both cases of OH^- diffusion through HA, the diffusion distances at the initial stage of dehydroxylation must be much further than those at higher conversion degrees, according to geometric knowledge. Both the diffusion distance and the low temperature can make the rate of OH^- diffusion low enough to restrict the overall dehydroxylation rate at stage 1. So process A could be interpreted into OH^- diffusion through HA.

Obviously, process B can be neither the dehydroxylation reaction ($2OH^- \rightarrow H_2O\uparrow + O^{2-}$), nor OHA lattice constitution, due to the great deviation of both activation energies. Also process B can not be the H_2O expulsion through product layer because the dimension of product layer is too limited to hinder H_2O expulsion and, therefore, influence the overall dehydroxylation rate at the initial stage. Consequently, the possible mechanism for process B should be OH^- anion debonding. In the lattice of HA, OH^- anion bonds with Ca^{2+} cation.[37] The bonding configuration of (OH)–Ca should be a kind of mixed bonding with both ionic and covalent characteristics. The bonding energies for ionic bonding are 600–1500 kJ/mol, as well as 100–800 kJ/mol for covalent bonding.[38] Interestingly the E value for process B, amounting to 530 kJ/mol, is less than the lower limitation of ionic bonding energies, as well as a bigger value in the range of covalent bonding energies. Such a result closely meets the mixed characteristics of (OH)–Ca bonding. So the E value for OH^- anion debonding from HA lattice by breaking (OH)–Ca bonding must be close to that of process B. According to above analysis, process B could be the process of OH^- anion debonding.

Table 1
Reported activation energies for the possible kinetic processes during the dehydroxylation of HA

No.	Kinetic processes	E (kJ/mol)	Ref.
1[a]	OH^--anion debonding from HA lattice in HA	Unknown	
2	OH^--anion diffusion through HA	230	[36]
3	$2OH^- \rightarrow H_2O\uparrow + O^{2-}$ at the reaction interface	251	[4]
4	H_2O expulsion through OHA or OA layer	Unknown	
5[a]	The lattice constitution of OA	440	[36]

[a] Its range of E value can be estimated according to the bonding characters.

3.2. Conversion stage 2 ($0.13 \leqslant \alpha < 0.7$, $764\ ^\circ C \leqslant T < 866\ ^\circ C$)

As for process C, it can be easily identified as OA lattice constitution, due to the obvious similarity between the values of both activation energies. With the proceeding dehydroxylation, the size of HA core keeps decreasing, therefore the diffusion distance, for OH^--anion to diffuse through HA, becomes shorter and shorter. It is rational that the process A becomes less kinetically important for dehydroxylation rate-controlling at the conversion stage 2, due to Arrhenius law. The overall mass loss rate is jointly regulated by OH^--anion debonding and OA lattice constitution. Trombe and Montel[39] demonstrated that the stage of temperature for OA stability is very narrow around 800–1050 °C. As marked with the dash lines in Fig. 3, this temperature range is corresponding to $0.3 \leqslant \alpha < 1$. Additionally, the critical value of x for preserving the HA lattice is reported to be 0.5.[9–10] These suggest OA becomes much more thermodynamically stable than HA in the range of $0.3 \leqslant \alpha < 1$, which includes the late half of stage 2, stage 3 and stage 4 of present study. Therefore, the lattice constitution of OA plays a more important role than OH^--anion debonding from the late half of stage 2.

3.3. Conversion stage 3 ($0.7 \leqslant \alpha < 0.8$, $866\ ^\circ C \leqslant T < 897\ ^\circ C$)

In stage 3 ($0.7 \leqslant \alpha < 0.8$), the dehydroxylation is kinetically controlled only by process C, OA lattice constitution by the migration of O^{2-} in the hydroxyl-depleted areas. According to the Arrhenius relation, the rate constant of the process B, OH^--anion debonding from HA lattice, at 866 °C is calculated to be 5.8×10^4 times higher than that at 680 °C, the initial temperature of process B. This result indicates that process B can not be a rate-controlling step of dehydroxylation at such a high temperature range.

3.4. Conversion stage 4 ($0.8 \leqslant \alpha < 0.98$, $897\ ^\circ C \leqslant T \leqslant 1080\ ^\circ C$)

At this stage, the sintering temperature could be high enough that both the OH^- debonding and diffusion are too fast to influence the overall dehydroxylation rate.

Table 2
Interpretation of the activation energies for the possible kinetic processes during the dehydroxylation of HA detected by the Ozawa–Flynn–Wall method

No.	Interpreted kinetic processes	α	E (kJ/mol)
A	OH^--anion diffusion through HA	$0.02 \leqslant \alpha < 0.13$	190
B	OH^--anion debonding from HA lattice in HA	$0.02 \leqslant \alpha < 0.7$	530
C	The lattice constitution of OA	$0.13 \leqslant \alpha < 0.98$	410
D	$2OH^- \rightarrow H_2O\uparrow + O^{2-}$ at the reaction interface	$0.8 \leqslant \alpha \leqslant 0.98$	235

By comparing the E values of process D with the reported values listed in Table 1, it is very close to the value of the activation energy of dehydroxylation reaction ($2OH^- \rightarrow H_2O\uparrow + O^{2-}$). Although the E value of process D has a good consistence with that of $2OH^- \rightarrow H_2O\uparrow + O^{2-}$, as well as there is no reported E value for H_2O expulsion through OA layer, the possibility of process D corresponding to H_2O expulsion through OA layer can not be excluded thoroughly. Based upon present-collected data, the rate-controlling processes might be lattice constitution of OA and $2OH^- \rightarrow H_2O\uparrow + O^{2-}$ at the interface of dehydroxylation, when dehydroxylation of HA reaches conversion stage 4.

It should be pointed out that there is merely about 80% HA transformed into OA at the end of the dehydroxylation of HA. In other words, there is 20% HA undehydroxylated, which will decompose at a higher temperature.[3–11] The interpreted results of four detected kinetic processes are listed in Table 2.

4. Conclusions

1. The dehydroxylation of commercial HA powder is a comprehensive chemical reaction, including four successive conversion stages corresponding to different kinetic mechanisms: stage 1 ($0.02 \leqslant \alpha < 0.13$), stage 2 ($0.13 \leqslant \alpha < 0.7$), stage 3 ($0.7 \leqslant \alpha < 0.8$), and stage 4 ($0.8 \leqslant \alpha \leqslant 0.98$).
2. According to the characteristics of the E–α plot of the dehydroxylation of commercial HA powder, there are four different kinetic processes identified with the activation energies of 200, 530, 410, and 235 kJ/mol, respectively, which possibly could be OH^--anion diffusion through HA, OH^--anion debonding from HA lattice, the lattice constitution of OA, and $2OH^- \rightarrow H_2O\uparrow + O^{2-}$ at the reaction interface.
3. It is suggested in this study that conversional stages 1, 2, 3, and 4 of dehydroxylation of HA are kinetically controlled by OH^--anion diffusion through HA and OH^--anion debonding from HA lattice, OH^--anion debonding and the lattice constitution of OA, the lattice constitution of OA, as well as the lattice constitution of OA and $2OH^- \rightarrow H_2O\uparrow + O^{2-}$ at the reaction interface, respectively.

References

1. Jarcho, M., Bolen, C. H., Thomas, M. B., Bobick, J., Kay, F. and Doremus, R. H., Hydroxyapatite synthesis and characterization in dense polycrystalline form. *J. Mater. Sci.*, 1976, **11**, 2027–2035.
2. Akoi, H., Karto, K., Ogiso, M. and Tabata, T., Sintered hydroxyapatite as a new dental implant material. *J. Dental Outlook*, 1977, **49**, 567–575.
3. Cihláø, J., Buchal, A. and Trunec, M., Kinetics of thermal decomposition of hydroxyapatite bioceramics. *J. Mater. Sci.*, 1999, **34**, 6121–6131.
4. Gross, K. A., Berndt, C. C., Stephens, P. and Dinnebier, R., Oxyapatite in hydroxyapatite coatings. *J. Mater. Sci.*, 1998, **33**, 3985–3991.
5. Zhou, J., Zhang, X., Chen, J., Zeng, S. and De Groot, K., High temperature characteristics of synthetic hydroxyaptite. *J. Mater. Sci.: Mater. in Medicine*, 1993, **4**, 83–85.
6. Liao, C., Lin, F., Chen, K. and Sun, J., Thermal decomposition and reconstitution of hydroxyapatite in air atmosphere. *Biomaterials*, 1999, **20**, 1807–1813.
7. Chen, J., Tong, W., Yang, C., Feng, J. and Zhang, X., Effect of atmosphere on phase transformation in plasma-sprayed hydroxyapatite coatings during heat treatment. *J. Biomater. Res.*, 1997, **34**, 15–20.
8. Locardi, B., Pazzaglia, U. E., Gabbi, C. and Profilo, B., Thermal behaviour of hydroxyapatite intended for medical applications. *Biomaterials*, 1993, **14**, 437–441.
9. Hartmann, P., Barth, S., Vogel, J. and Jäger, C., Investigations of structural changes in plasma-sprayed hydroxy apatite coatings. *Applied Mineralogy*, 2000, **1**, 147–150.
10. Hartmann, P., Jäger, C., Barth, S., Vogel, J. and Meyer, K., Solid state NMR, X-ray diffraction, and infrared characterization of local structure in heat-treated oxyhydroxyapatite microcrystals: an analog of the thermal decomposition of hydroxyapatite during plasma-spray procedure. *J. Solid State Chem.*, 2001, **160**, 460–468.
11. Chai, C. and Ben-Nissan, B., Thermal stability of synthetic hydroxyapatites. *Inter. Ceramic Monographs*, 1994, **1**, 79–85.
12. Ozawa, T., A new method of analyzing thermogravimetric data. *Bull. Chem. Soc. Jpn*, 1965, **38**, 1881–1885.
13. Flynn, J. H. and Wall, L. A., A quick, direct method for the determination of activation energy from thermogravimetric data. *Polym. Lett.*, 1966, **4**, 323–328.
14. ASTM Test Method E1641, *Standard Test Method for Decomposition Kinetics by Thermogravimetry*. ASTM Book of Standards 14.02, American Society for Testing and Materials, 1994, 1042–1046.
15. Brown, M. E., Maciejewski, M. and Vyazovkin, S., Computational aspects of kinetic analysis Part A: the ICTAC kinetics project-data, methods and results. *Thermochimica Acta*, 2000, **355**, 125–143.
16. Vyazovkin, S., Computational aspects of kinetic analysis Part C: the ICTAC kinetics project—the light at the end of the tunnel?. *Thermochimica Acta*, 2000, **355**, 155–163.
17. Maciejewski, M., Computational aspects of kinetic analysis Part B: the ICTAC kinetics project—the decomposition kinetics of

calcium carbonate revisited, or some tips on survival in the kinetic minefield. *Thermochimica Acta*, 2000, **355**, 145–154.
18. Burnham, A. K., Computational aspects of kinetic analysis Part D: the ICTAC kinetics project—multi-thermal-history model-fitting methods and their relation to isoconversional methods. *Thermochimica Acta*, 2000, **355**, 165–170.
19. Roduit, B., Computational aspects of kinetic analysis Part E: the ICTAC kinetics project—numerical techniques and kinetics of solid state process. *Thermochimica Acta*, 2000, **355**, 171–180.
20. Koga, N. and Criado, J. M., Kinetic analyses of solid-state reactions with a particle-size distribution. *J. Am. Ceram. Soc.*, 1998, **81**, 2901–2909.
21. Vyazovkin, S. and Wight, C. A., Model-free and model-fitting approaches to kinetic analysis of isothermal and nonisothermal data. *Thermochim. Acta*, 1999, **340/341**, 53–68.
22. Vyazovkin, S. and Wight, C. A., Isothermal and nonisothermal kinetics of reactions of solids. *Int. Rev. Phys. Chem.*, 1998, **17**, 407–433.
23. Vyazovkin, S. and Wight, C. A., Isothermal and nonisothermal reaction kinetics in solids: a search for consensus. *J. Phys. Chem.*, 1997, **A101**, 8279–8284.
24. Vyazovkin, S., Kinetic concepts of thermally stimulated reactions in solids: a view from a historical perspective. *Int. Rev. Phys. Chem.*, 2000, **19**, 45–60.
25. Vyazovkin, S., A unified approach to kinetic processing of non-isothermal data. *Int. J. Chem. Kinet.*, 1996, **28**, 95–101.
26. Vyazovkin, S., Conversion dependence of activation energy for model DSC curves of consecutive reactions. *Thermochim. Acta*, 1994, **236**, 1–13.
27. Wang, T., Lu, Y. X., Zhu, M. L. and Zhang, J. S., Identification of the comprehensive kinetics of thermal explosion synthesis Ti + 3Al→TiAl3 using non-isothermal differential scanning calorimetry. *Mater. Lett.*, 2002, **54**, 284–290.
28. Wang, G. and Dahms, M., Synthesizing gamma-TiAl alloys byreactive powder processing. *JOM*, 1993, **45**, 52–56.
29. Furedi-Milhofer, H., Hlady, V., Baker, F. S., Beebe, R. A., Wikhom, N. W. and Kittelberger, J. S., Temperature-programmed dehydration of hydroxyapatite. *J. Colloid Interface Sci.*, 1979, **70**, 1–9.
30. Skinner, H. C. W., Kittelberger, J. S. and Beebe, R. A., Thermal instability in synthetic hydroxyapatites. *J. Phys. Chem.*, 1975, **79**, 2016–2019.
31. Owada, H., Yamashita, K. and Kanazawa, T., High-temperature stability of hydroxyl ions in yttrium-substituted oxyhydroxyapatites. *J. Mater. Sci. Lett.*, 1990, **9**, 26–28.
32. Larmas, M. A., Hayrynen, H. and Lajunen, L. H. J., Thermogravimetric studies on sound and carious human enamel and dentin as well as hydroxyapatite. *Scand. J. Dent. Res.*, 1993, **101**, 185–191.
33. Adolfsson, E., Nygren, M. and Hermansson, L., Decomposition mechanisms in aluminum oxide–apatite systems. *J. Am. Ceram. Soc.*, 1999, **82**, 2909–2912.
34. Riboud, P. V., Composition et Stabilité des Phases a Structure d'Apatite dans le Systeme CaO–P_2O_5–Oxyde de Fer–H_2O a Haute Temperature. *Ann. Chim.*, 1973, **8**, 381–390.
35. van Raemdonck, W., Ducheyne, P. and de Meester, P., Calcium phosphate ceramics. In *Metal and Ceramic Biomaterials, Vol. II*, ed. P. Ducheyne and G. W. Hastings. CRC Press, Boca Raton, FL, 1984.
36. Gross, K. A., Gross, V. and Berndt, C. C., Thermal analysis of amorphous phases in hydroxyapatite coatings. *J. Am. Ceram. Soc.*, 1998, **81**, 106–112.
37. Narassarju, T. S. B. and Phebe, D. E., Review some physicochenical aspects of hydroxyapatite. *J. Mater. Sci.*, 1996, **31**, 1–21.
38. Callister, W. D., *Materials Science & Engineering: An Introduction*, 4th edn. John Wiley & Sons, New York, 1997.
39. Trombe, J. C. and Montel, G. J., Some features of the incorporation of oxygen in different oxidation states in the apatitic lattice—I. *Inorg. Nucl. Chem.*, 1977, **40**, 15–21.